

# Study of the utility of PET image in refractory epilepsy

Author: Maite Fabregat Frances.

*Facultat de Física, Universitat de Barcelona, Diagonal 645, 08028 Barcelona, Spain.\**

Advisor: Domènec Ros.

**Abstract:** The surgical removal of the epileptogenic region is considered as a possible treatment in intractable partial epilepsy. To guarantee surgery to be successful, an accurate localization of epileptogenic focus is crucial. A new proposal for its location is described and discussed. Six patients were used in the evaluation and the results were compared with other techniques routinely used for this purpose. All the processed studies showed a good agreement. As a result, it is seen great promise in this new methodology and further evaluation makes sense.

## I. INTRODUCTION

Epilepsy is a neurological disorder that consists of a tendency to suffer discontroled and anormal activation of neuronal groups in the brain. It affects 1-2% of the population, around 50 million people worldwide. This disease can be classified into two major types: partial or generalized epilepsy. In partial epilepsy the activation is caused by a specific and located group of neurons which is called *epileptic focus* (EP). On the contrary, generalized epilepsy is defined as difuse. Between 25-30% of patients with epilepsy do not respond to antiepileptic treatment. They are said to suffer *refractory epilepsy*. In these cases, the exeresis of the epileptogenic area without causing a permanent neurological deficit is considered [2].

A variety of diagnostic techniques are used to locate the EP. Some of them are the *intracranial electroencephalogram* (EEG), *Magnetic Resonance Imaging* (MRI), *Single Photon Emission Computed Tomography* (SPECT) or *Positron Emission Tomography* (PET) [8]. Both PET and SPECT are Nuclear medicine techniques. Nuclear medicine uses *radiopharmathecials* in order to achieve internal body images. The radiopharmathecials is a compound of a radionucleid bounded to a targetting molecule that is designed to interact with specific body's molecules. As a consequence, after a certain period of time, a radiotracer distribution is fixed inside the body. This function maps some physiological property.

SPECT is a nuclear medicine tomography imaging technique that is based on the detection of the gamma rays produced in the nuclear decay [4]. Cerebral blood flow (CBF) is measured in epilepsys studies.

PET is another tomography imaging technique based on the detection of pairs of gamma rays that come from the annihilation of the positron emitted by the nuclear decay of the radiotracer [5]. In epilepsy, the PET radiotracers are designed to evaluate the glucose metabolism.

Image processing refers to the set of transformations that are applied to the achieved image in order to empha-

size a feature of the functional information of the image that is interesting for the diagnosis.

During an epileptogenic seizure, also called ictal state, both regional CBF and metabolism are increased in the ER. In contrast, interictal state refers to a seizure-free period and shows a decrease of both features.

Visual comparison of Ictal SPECT and Interictal SPECT was used in the detection and location of the EF. This comparison can be difficult due to intensity and orientation differences [7].

Subtraction ictal SPECT co-registered to MRI (SISCOM) [3] is a methodology that fusions both ictal and interictal SPECT images to the MRI anatomical image, normalizes and subtracts information of the differences with a threshold in order to facilitate the visual evaluation. SISCOM processing is commonly divided into four steps: SPECT-SPECT (S-S) registration, intensity normalization, subtraction and SPECT-MRI (S-M) registration .

Direct visual comparison shows a sensitivity of 39.2% compared with 88.2% when using SISCOM images [3].

There is more reduction in regional cerebral glucose metabolic uptake than in CBF in the epileptogenic region. The sensitivity of interictal PET images is higher than that of interictal SPECT. An exemple is shown in figure 1. Therefore, the feasibility of substituting the Interictal SPECT image in SISCOM analysis for the PET image was raised.

This is not only interesting because of the possibility of a better detection but because the acquisition of the PET Interictal image is already performed inasmuch as it is used itself as a diagnosis method [6]. The aim of this bachelor thesis was to perform and discuss this substitution.

## II. MATERIAL AND METHODS

Data from 6 anonymised studies from Epilepsy Unit database of the *Hospital Clínic de Barcelona* were used to evaluate the hypothesis. Selection was performed so that Interictal SPECT, Ictal SPECT, Interictal PET and MRI images were available. The features of the acquisition are

---

\*Electronic address: maite@fabregat.eu

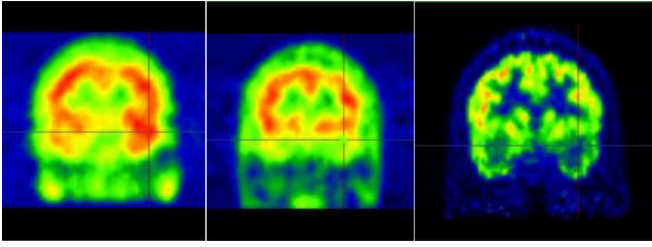


FIG. 1: Ictal, Interictal SPECT and Interictal PET.

described in table I.

	SPECT	CT-PET
Radiopharmaceutical	$[^{99m}\text{Tc}] - \text{HMPAO}$	$[^{18}\text{F}] - \text{FDG}$
Injected dosis	925MBq	5MBq/Kg
Imaging System	dual-head <i>Infinia<sup>TM</sup> Hawkeye<sup>TM</sup></i> 4 from GE Healthcare with low energy high resolution parallel-hole collimators.	Biograph MCT Siemens equipment.
Reconstruction	Filtered Back Projection (FBP) algorithm with Butterworth filter ( $f = 0.42\text{cm}^{-1}$ ; order 5.8)	Ordered Subsets Expectation Maximization (OSEM)(16 subsets, six iterations)
Matrix dimensions	128x128xz, $z \sim 60$	400x400x148
Voxel size	3.32x3.32x3.32	2.4x2.4x2.1

TABLE I: Main properties of the SPECT and PET acquisitions.

T1-weighted MRI studies were performed in a 3T unit (Trio SIEMENS) with a specific protocol: Coronal 3D MPRAGE (TR 2000 ms; TE 2.98 ms, 0.9mm slice thickness). The sequence was acquired parallel to the long axis of hippocampus and the full brain was covered.

PET images were processed using different tools. MATLAB and Statistical Parametrical Mapping (SPM8) [9] software are some examples. The SISCOM methodology for both Interictal-Ictal SPECT and Interictal PET-Ictal SPECT evaluation were performed using the SISCOM analysis plug-in of FocusDET [1] which is implemented in GIMIAS [10].

### III. SUBSTITUTION OF INTERICTAL SPECT FOR PET IMAGE IN THE SISCOM ANALYSIS

PET and SPECT images exhibit numerous differences among themselves due to the acquisition systems used in each one and the physical laws that reign each process.

Before substitution in the SISCOM analysis is made, it is necessary to consider a normalization process so that both images show more similar features. It was chosen

to modify the PET image among other options.

All procedures that were performed to analyse and reduce these differences were based on the comparison of Interictal SPECT and Interictal PET images.

#### A. Need of processing

SPECT and PET are usually obtained using different image format and matrix size. In order to substitute interictal SPECT successfully, PET images were pre-processed in order to have the same characteristics: the SPECT images, i.e. 128x128 matrix size, 3.32x3.32x3.32  $\text{mm}^3$  voxel size, 4 bytes float data format. This transformation was performed with SPM coregister tool using default values.

The input images of SISCOM Analysis plug-in must have the same number of voxels in two of the three dimensions. In addition, same cubic-voxel size is needed.

#### B. Count number normalization

The total number of detected photons in SPECT and PET is different. In order to correct this, each voxel of the PET images were multiplied by a factor  $a$ . This factor was calculated using equation 1

$$a = \frac{\sum_{i=1}^{N_x} \sum_{j=1}^{N_y} \sum_{k=1}^{N_z} f(x_i^s, x_j^s, x_k^s)}{\sum_{i=1}^{N_x} \sum_{j=1}^{N_y} \sum_{k=1}^{N_z} g(x_i^p, x_j^p, x_k^p)} \quad (1)$$

where  $f(x_i^s, x_j^s, x_k^s)$  and  $g(x_i^p, x_j^p, x_k^p)$  are the PET and SPECT images, respectively. Intensity normalization factors ranging between  $3.1 \cdot 10^{-3}$  and  $5.5 \cdot 10^{-3}$  were obtained.

#### C. Resolution

Let  $\rho(x', y', z')$  be the density distribution of the radiotracer and  $f(x, y, z)$  be the resulting acquired image. Assuming that the imaging system behaves as a linear system, it can be written

$$f(x, y, z) = h(x', y', z') \otimes \rho(x', y', z')$$

where  $h$  is called the *Point Spread Function* (PSF) of the acquisition system and  $\otimes$  means convolution. The degradation that the real image  $\rho$  suffers in the acquisition is then the PSF. In order to be comparable, both images need to exhibit similar degradations. A convolution between PET images and the inverse PSF of the PET acquisition system followed by a convolution with the SPECT PSF leads to a filtered PET image with a degradation equivalent to that of interictal SPECT.

The Time-Frequency convolution theorem

$$f \otimes g \Leftrightarrow \mathcal{F}(f)\mathcal{F}(g)$$

is used in order to apply the filter in the Fourier space due to its faster computational implementation.

The Discrete Fourier transform

$$F\left(\frac{n}{N\Delta u}\right) = \sum_{k=0}^{N-1} f(k\Delta u) e^{-i2\pi nk/N} \quad n = 0, 1, \dots, N-1 \quad (2)$$

was calculated using the 3D Fast Fourier Transform (FFT) algorithm implemented in MATLAB, *ttfn*, after a padding so that the matrix to be transformed had dimensions of powers of 2, which accelerates the FFT algorithm.

The Fourier transform (FT) of the image was assumed to have spherical symmetry so that every pixel with the same distance to the centre of the Fourier Transform represent the same frequency.

A program in MATLAB that sums over both angles and calculates the average value was implemented. The absolute frequency was calculated, so the distance to the center of the Fourier Transform of a voxel  $(i, j, k)$  of the FT was

$$w(i, j, k) = \sqrt{\left(\frac{i}{N_x\Delta u}\right)^2 + \left(\frac{j}{N_y\Delta v}\right)^2 + \left(\frac{k}{N_z\Delta w}\right)^2}$$

Experimental PSF images were obtained from the SPECT and the PET acquisition system. The frequency spectrums of both images were calculated as described above and can be seen in figure 2.

	SPECT PSF	PET PSF
N	128x128x128	400x400x148
Voxel size (mm)	3.32x3.32x3.32	1.02x1.02x1.50
Frequency Interval ( $10^{-3} \text{ mm}^{-1}$ )	5.21	2.35
Nyquist Frequency ( $10^{-1} \text{ mm}^{-1}$ )	1.51	3.33

TABLE II: Frequency interval and Nyquist frequency for SPECT PSF and PET PSF. The frequency interval was calculated using  $\min(\frac{1}{2N_i\Delta u_i})$ ,  $i = 1, 2, 3$ , index  $i$  referring to the 3 dimensions,  $N$  to the number of samples and  $\Delta u$  to the length of the voxel side. The Nyquist Frequency  $\min(\frac{1}{2\Delta u_i})$

The following function was proposed as a fitting model for both obtained amplituds of the FT and a fit was performed using MATLAB *cftool* tool.

$$H(w) = a_1 e^{-\left(\frac{w-b}{c}\right)^2} + a_2 \frac{1}{1 + \left(\frac{w}{w_0}\right)^{2n}} \quad (3)$$

The values obtained for the coefficients are shown in table III. The  $R^2$  correlation coefficient was in the two

cases of 1. All the frequencies greater than the nyquist frequency were not considered for the ajustment.

	$a_1$	$b$	$c$
SPECT	$1,533 \cdot 10^6$	-0,0004	0,036
PET	$1,126 \cdot 10^8$	-0,0042	0,091
	$a_2$	$w_0$	$n$
SPECT	$1,149 \cdot 10^6$	0,0419	2,86
PET	$1,017 \cdot 10^7$	0,1629	3,34

TABLE III: Coefficients obtained by fitting the function  $H$  to the SPECT and PET images with 95% confidence bounds

Finally the filter to apply to the PET image was

$$H_f(w) = \frac{H_{SPECT}(w)}{H_{PET}(w)}$$

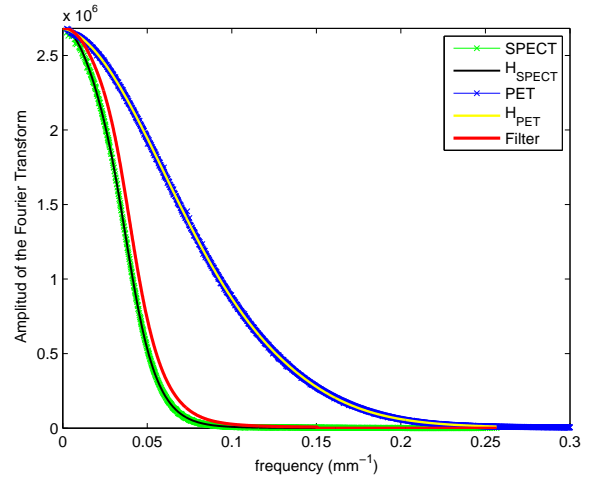


FIG. 2: Spectral components of the PET and SPECT PSF and the obtained filter scaled to the same value

The obtained function  $H$  was evaluated using the *feval* MATLAB function at the domain of the SPECT frequencies. The filter was reconstructed assuming spherical symmetry and applied to the PET images. The results are shown in Figure 3. An expert reaffirmed the compatibility of the resolution of both images. Despite this, the noise in SPECT image is higher than in the smoothed PET image.

#### IV. RESULTS

Due to the lack of appropriate label, we will call this method "PSISCOM". In order to evaluate its accuracy, an expert in EF location with SISCOM methodology reported the position of the EF in the 6 studies. The reported locations were compared with the deduced one

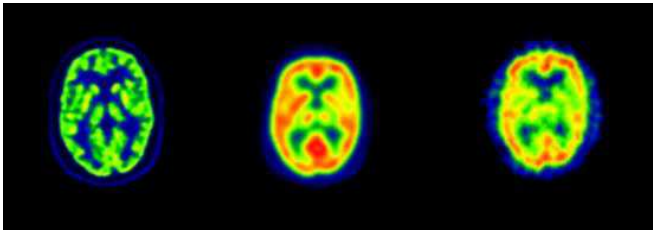


FIG. 3: Axial section of an original PET, preprocessed PET and Interictal SPECT image from left to right.

Patient	PSISCOM	SISCOM
1	EP in Frontal I, insula and cerebellum	EP in Frontal I, insula and cerebellum
2	Right Temporal lobe	Right Temporal lobe
3	Left Temporal lobe	Left Temporal lobe
4	Negative	Negative
5	Negative, easier evaluation	Negative
6	Both temporal, increased uptake of the left side.	More noise in Frontal lobe.

TABLE IV: Comparison between PSISCOM and SISCOM methodology in the EF location.

using SISCOM Analysis. Table IV summarizes the key points of the results.

Some recurrent features were worth mentioning. Negative cases were better seen. Cerebellum zone can not be evaluated with PSISCOM inasmuch as the systematic decreased uptake that appears in the PET image. A new mask should be generate as in using the SPECT mask for the PET image within the SISCOM analysis artifactual extra cerebral activity appears in the border. This can be seen in figure 4.

We can see that the EF is located at the same regions using PSISCOM as SISCOM analysis, thereby validating the proof of concept inherent in this study.

## V. CONCLUSIONS

The hypothesis of substituting interictal PET in the SISCOM analysis has been evaluated. The proof of concept using interictal PET or interictal SPECT led to

the same localization of the epileptogenic area. These highly promising results show the interest of a further study oriented to the complete validation of the PSISCOM methodology with a larger database of patients and using the results of the surgery as the gold standard.

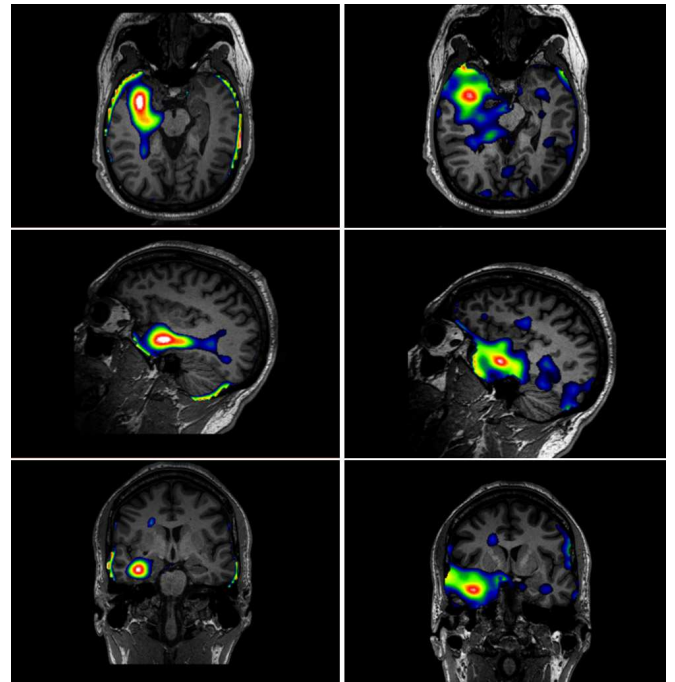


FIG. 4: Outcomes of PSISCOM (left) and SISCOM (right).

## Acknowledgments

I would like to thank my advisors Dr. Ros and Dra. Puig for giving me the opportunity of working in this stimulating area and for his valuable time and patience on helping me to solve all the problems I have encountered testing this hypothesis. I also want to acknowledge Dr. Pavia and Dr. Massaneda for their guideness at every moment and *Hospital Clínic* for the studies provided and Dr. Setoain for the visual evaluation.

I also want to thank my family for their advises and support, specially my sister Blanca for helping me with the medical issues.

- 
- [1] Mart Fuster, Berta. *Image processing of emission tomography studies in refractory epilepsy*. (PhD Thesis Universitat de Barcelona). (2013).
- [2] Beleza P. "Refractory Epilepsy: A Clinically Oriented Review". *European Neurology*. **62**: 65-71 (2009).
- [3] OBrien, T.J., So, E.L., Mullan, B.P. et al, D. "Subtraction ictal SPECT co-registered to MRI improves clinical usefulness of SPECT in localizing the surgical seizure fo-

cus". *Neurology*. **50**: 445454 (1998).

- [4] Wernick M. , Aarsvold N. *Emission tomography: The fundamentals of PET and SPECT*. -(Elsevier Science, Oxford, 1st ed., 2004).
- [5] Gopal B. Saha *Basics of PET Imaging Physics, Chemistry and Regulations*. (Springer-Verlag New York, 2010).
- [6] Manguiere, F. and Ryvlin, P. "The role of PET in presurgical assessment of partial epilepsies". *Epileptic Disor-*

- ders, **6**: 1841-1847 (2004).
- [7] C. la Fougère, A. Rominger, D. Frster, J. Geisler, P. Bartenstein. "PET and SPECT in epilepsy: A critical review". *Epilepsy and Behavior* **15**: 50-55 (2009).
- [8] X. Setoain, M. Carreño, J. Pavía, B. Martí-Fuster, F. Campos, F. Lomeña. "PET and SPECT in epilepsy". *Revista Española de Medicina Nuclear e Imagen Molecular*. **33**: 165-174 (2014).
- [9] <http://www.fil.ion.ucl.ac.uk/spm/software/spm8/>
- [10] [www.gimias.org](http://www.gimias.org)